1991, *24*, 6863. (b) Imori, T.; Woo, H.-G.; Walzer, J. F.; Tilley, T. D. *Chem. Mater.* **1993**, *5*, 1487.
8. (a) Harrod, J. F. in *Transformation of Organometallics into Common and Exotic Materials: Design and Activation*; Laine, R. M., Ed.; NATO ASI Series E.: Appl. Sci. no. 141; Martinus Nijhoff Publishers: Amsterdam, 1988; p 103. (b) Mu, Y.; Harrod, J. F. in *Inorganic and Organometallic Polymers and Oligomers*; Harrod, J. F.; Laine, R. M., Eds.; Kluwer Academic Publishers: Dordrecht, 1991; p 23.
9. Woo, H.-G.; Harrod, J. F. Manuscript in preparation.
10. Tilley, T. D. *Acc. Chem. Res.* **1993**, *26*, 22.
11. (a) Wolff, A. R.; Nozue, I.; Maxka, J.; West, R. *J. Polym. Sci., Part A: Polym Chem.* **1988**, *26*, 701. (b) Maxka, J.; Mitter, F. K.; Powell, D. R.; West, R. *Organometallics* **1991**, *10*, 660.
12. (a) Banovetz, J. P.; Stein, K. M.; Waymouth, R. M. *Organometallics* **1991**, *10*, 3430. (b) Corey, J. Y.; Huhmann, J. L.; Zhu, X.-H. *Organometallics* **1993**, *12*, 1121. (c) Li, H.; Butler, I. S.; Harrod, J. F. *Organometallics* **1993**, *12*, 4553.
13. Campbell, W. H.; Hilty, T. K. *Organometallics* **1989**, *8*, 2615.
14. Lee, B. W.; Yoo, B. R.; Kim, S.-I.; Jung, I. N. *Organometallics* **1994**, *13*, 1312.
15. Li, H.; Gauvin, F.; Harrod, J. F. *Organometallics* **1993**, *12*, 575.

The Adsorption Energetics and Geometry of Ketene Physisorbed on Ag(111)*

Jung-Soo Kim and Hai-Lung Dai

Department of Chemistry and Laboratory for Research on the Structure of Matter, University of Pennsylvania, Philadelphia, PA 19104, U. S. A.

Received October 24, 1994

Ketene (CH_2CO) adsorption on Ag(111) has been studied in ultrahigh vacuum using electron energy loss spectroscopy and temperature programmed desorption. Ketene adsorbs molecularly on Ag(111) at temperatures below 126 K. The coverage increases linearly with exposure until saturation. No multilayer formation and no shift in desorption temperature with coverage were observed, indicating a lack of attractive interaction between adsorbate molecules. The desorption activation energy is estimated to be 7.8 kcal/mol by assuming first order kinetics and a pre-exponential factor of 10^{13} sec^{-1}. The adsorption geometry of ketene on the surface is determined from the relative intensities of the vibrational energy loss peaks. The CCO axis of CH_2CO is found to be almost parallel to (~4° away from) the surface and the molecular plane is almost perpendicular to the surface (~3° tilt).

Introduction

Ketene, CH_2CO, is a convenient source of methylene which has been postulated as an important intermediate in the Fischer-Tropch synthesis of hydrocarbons.[1] To isolate and unambiguosly identify methylene, an unstable species, on transition metal surfaces has been the goal for a number of experiments under ultrahigh vacuum conditions.[2,3] As a precusor to methylene, ketene adsorption on single crystal surfaces needs to be characterized and understood.

McBreen *et al.*[4] observed that ketene adsorbs molecularly on Fe(110) at 120 K, but dissociates to CO and bridge-bonded methylene at 390 K. On the other hand, Radloff *et al.*[5] reported that on Pt(111) at low exposures, ketene adsorbs dissociatevely at 100 K. The only products found by temperature programmed desorption (TPD) were H_2 and CO, with carbon left on the surface. At high exposures, ketene and ethylene were detected in the TPD experiment in addition to H_2 and CO. Similar to the Pt(111) observations, ketene adsorption at 105 K on Ru(001)[6] occurs both molecularly and dissociatevely depending on the exposure. The desorption products here are H_2, CO, and CO_2 with no hydrocarbon detected.

One of the main reasons for studying physisorbed or weakly chemisorbed molecule is that properties of the adsorbed molecules can be compared with the properties of the gas-phase molecules. Insight into the nature of the adsorbate-substrate interaction and molecular processes on surfaces can be gained from such comparisons. In particular, surface photochemical reaction of a weakly adsorbed molecule may be similar to gas-phase reactions in terms of mechanism and energetics[7~9] provided that the surface only weakly perturbs the molecular properties.

A TPD study would allow the determination of adsorption energy. The extent of pertubation of the adsorbate molecules by the surface can be further revealed from the change of

*This article is dedicated to professor Woon-Sun Ahn, to whom Jung-Soo Kim is indebted for her graduate education and scientific developments, for commemorating the occassion of his retirement.

energies of the vibrational and electronic states, which can be measured by the electron energy loss spectroscopy (EELS), in comparison to those of the isolated molecules.

The orientation of a molecule physisorbed on the metal surface can be determined in principle from the vibrational transition intensities. On metal surfaces, these intensities in the infrared region are directly related to the square of the projection of the transition dipoles onto the surface normal. Although many EELS studies have used the relative intensities to qualitatively estimate the adsorbate orientation, there have been only a few quantitative attempts to extract orientation angles.[10~12] A quantitative characterization of the adsorption geometry of formaldehyde on Ag(111) has been reported[13] from EELS and TPD data. It has been determined that H_2CO weakly binds (~6 kcal/mol) to the Ag(111) surface in a geometry that the CO axis of formaldehyde is tilted away from the surface normal by 57° with a slight rotation of the molecular plane from the horizontal configuration. It was speculated that such an adsorption geometry is a result of the balance between the oxygen n orbitals-surface and the CO π orbital-surface interactions. The ketene molecule has a C=C chromophore in addition to the C=O chromophore. The additional C=C π orbital-surface interaction should make the C=C=O axis tilt farther away from the surface normal. In this work, we examine the adsorption energetics and geometry of ketene on Ag(111) at liquid nitrogen cooled temperatures. The adsorption geometry of ketene on Ag(111) will be elucidated from high resolution electron energy loss spectra while the data from TPD spectra will be used to deduce the adsorption energetics.

Experimental

The experiments were performed in an ion-pumped ultra-high vacuum (UHV) chamber with a base pressure of 1×10^{-10} Torr. The UHV chamber was equipped with an electron energy loss spectrometer (McAllister Technical Servies) for vibrational spectroscopy. All high resolution EELS were taken with an electron beam energy of 5.0± 0.1 eV. The spectral resolution is about 12 meV as full width at half maximum. The incident angle of the EELS electron beam was 65 degree with respect to the surface normal. The chamber also has a mass spectrometer (UTI 100C) with Ir filaments housed in a gold-plated stainless steel nose cone for temperature programmed desorption studies and background gas analysis.

The Ag(111) crystal was mounted on a resistive heating unit (Spectra Mat) with tantalum clamps. The crystal surface with 15 mm diameter was cleaned before each experiment by two cycles of Ne^+ sputtering and annealing to 730 K. The crystal could be cooled by thermal contact with cryostat (R. G. Hansen) to 87 K using liquid nitrogen or to 43 K using liquid helium. The temperature was measured by a chromel-alumel thermocouple spot welded to one of the clamps. The surface order and cleanness was verified by low energy electron diffraction (LEED) and EELS.

The ketene gas was prepared from pyrolysis of acetic anhydride vapor in a evacuated quartz tube maintained at about 780 K. The gas effluent of the quartz tube was passed through a trap at 196 K to condense both acetic acid and the residual acetic anhydride. Ketene was then collected in a second trap at 77 K, and subsequently transfered to a finger tube. Before dosing, the gas line was rinsed with ketene gas. Ketene was dosed by backfilling the chamber through a varible leak valve with the crystal held at around 87 K. Exposures were reported in Langmuirs ($1L=10^{-6}$ Torr-sec) with the pressure monitered by an ion gauge 0.3 m away from the sample surface. During the TPD experiment, the crystal was biased at −67.7 V to repel electrons emitted from the mass spectrometer filament. Without the biased voltage, electrons emitted from the filament may reach the surface and induce reactions of the adsorbate. The application of the biased voltage should not influence the TPD experiment of neutral species. For comparison with EEL spectra, the IR absorption spectra of 200 mTorr ketene gas in a 10 cm cell have been recorded by using a FTIR (Bruker IFS88) at 2 cm^{-1} resolution.

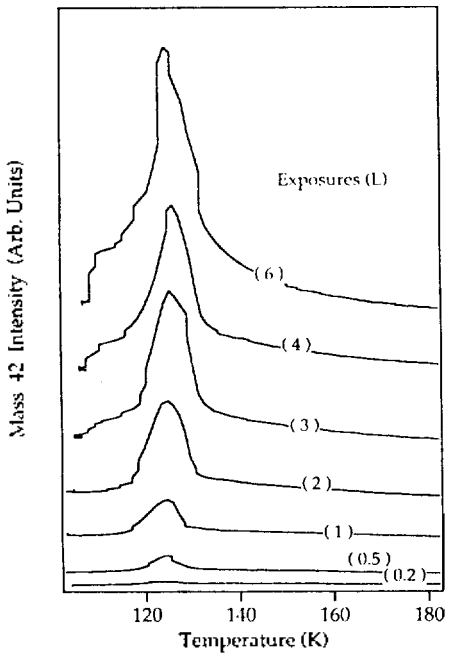

Figure 1. Temperature programmed desoption spectra (mass 42, 1 Ks^{-1}) for 0.2 L~6 L CH_2CO exposure on Ag(111).

Result and Analysis

Desorption and Adsorption Energetics. The TPD experiments of ketene initially adsorbed on Ag(111) at 87 K were performed up to 710 K. A linear heating rate of 1.0 Ks^{-1}, achieved by computer conrtrol, was used. None of the C_1 through C_4 hydrocarbons other than the ketene molecular fragments generated in the mass spectromer were detected regardless of the ketene exposures from 0.1 L to 12 L. Figure 1 shows a series of TPD spectra at mass 42 for ketene adsorbed on a clean Ag(111) surface with exposure ranges from 0.2 L to 6 L.

Only one desorption peak at 126 K, which corresponds to desorption of the ketene molecule, appears. At higher exposures of ketene, no additional peak appears below the 126 K peak, indicating no second layer formation. This is true even down to the liquid helium cooled 43 K. Figure 2 shows the integrated area of the TPD mass 42 peak as a function of exposure (L_{exp}). The integrated TPD area appears to satu-

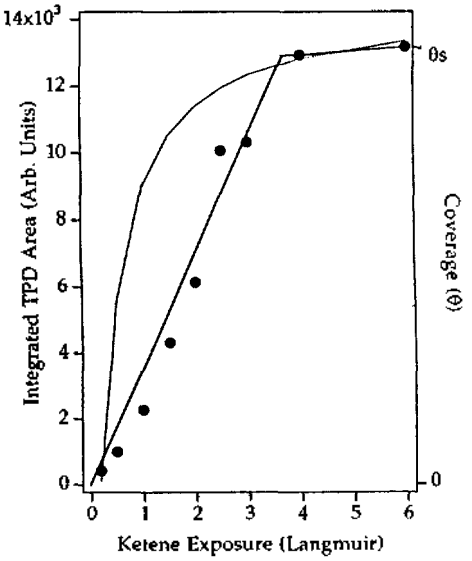

Figure 2. Integrated TPD area of the mass 42 peak as a function of ketene exposures. The curved line represents the fit to Langmuir kinetics model. The straight line for $0 \le L_{exp} \le 3.66$ L is $\theta = 0.274\ L_{exp}\theta_S$, where θ_S is the saturation coverage defined by the coverage at 6 L exposure.

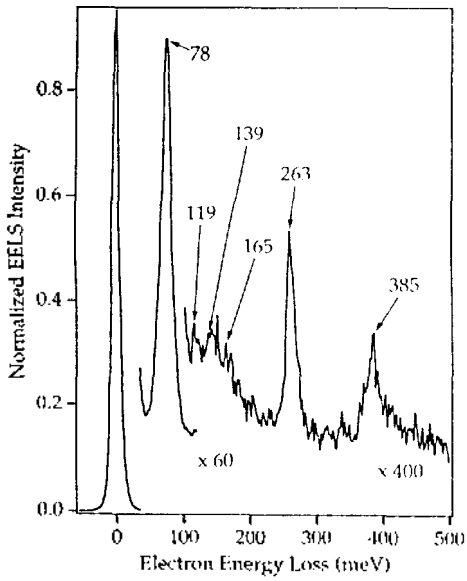

Figure 3. Vibrational EEL spectra for CH_2CO (2 L exposure) on Ag(111) at 87 K.

rate at ~4 L. The experimental data was first compared with the Langmuir kinetics model by fitting to the $\theta = [KL_{exp}/(1+KL_{exp})]\theta_S$ relationship. The TPD peak area is linearly proportional to the coverage θ on the surface. It was found that the data points do not agree with the Langmuir adsorption kinetics model. In fact, the presaturation points can be well represented by a linear relationship between coverage and exposure, Figure 2. By setting the coverage at 6 L as the saturation coverage θ_S, we obtain a calibration for coverage *vs.* exposure of

$$\theta = 0.274\ L_{exp}\theta_S,\ L_{exp} \le 3.66\ L. \quad (1)$$

This linear adsorption behaviour implies a nonconventional adsorption mechanism.

There is no discernable shift of the desorption temperature as well as narrowing of the desorption peak with increasing exposure in Figure 1. Normally, in a situation where there is attractive interaction between the adsorbate molecules, the desorption peak shifts to a higher temperature and the peak becomes narrower as the coverage increases.[14,15] Thus, it appears that there is no discenable attractive interaction between ketene adsorbates. This observation and interpretation is consistent with the observation of the lack of formation of second layer adsorption, which also indicates a lack of attractive interaction between the first layer and subsequently adsorbed molecules. In fact, the lack of second layer formation at 87 K supports that the inter-molecular interaction is of a repulsive nature. This conjecture is consistent with the observation of the linear relationship between coverage and exposure, which is similar to that of CO on Cu[16-18] where repulsive inter-adsorbate interaction was detected.[18]

Assuming first order kinetics for ketene adsorption and a pre-exponential factor of 10^{13} s^{-1},[19] we calculate from the 126 K desorption temperature the desorption activation energy as 7.8 kcal/mol. This activation energy value characterizes the ketene adsorption as physisorption.

Table 1. Assignment of the vibrational EELS peaks for CH_2CO adsorbed on Ag(111) at 87 K, and comparison with the gas-phase vibrational transition energies

Assignment	Adsorbed on Ag(111) (meV)	Gas-phase (meV)
ν_1 CH_2 symmetric stretch	385*	380.6
ν_2 CO stretch	263	266.8
ν_3 CH_2 scissoring	165	172
ν_4 CC stretch	139	139
ν_5 CH_2 wagging	78*	73
ν_6 CCO out-of-plane bend	78*	65
ν_7 CH_2 asymmetric stretch	385*	392
ν_8 CH_2 rocking	119	121
ν_9 CCO in-plane bend	—	54

*: unresolved peak. —: undetected.

It is revealing to compare the adsorption energetics of ketene to that of formaldehyde, both on Ag(111). The formaldehyde desorption temperature is lower (106 K), but the inter-formaldehyde adsorbate interaction is attractive, inducing island formation in below-saturation submonolayer coverages and the second layer adsorption.[13]

Vibrational spectroscopy. The nature of ketene adsorption is further characterized by electron energy loss spectra. Vibrational EEL spectra of 2 L exposure of ketene on Ag(111) at 87 K is shown in Figure 3. The spectrum is assigned to molecularly adsorbed CH_2CO. The peak assignments, made by comparison with the gas-phase IR spectra,[20] are presented in Table 1. The major EEL peak is at 78 meV, which is a mixture of CH_2 wagging and CCO out-of-plane bending bands. The EEL peak at 263 meV is from CO stret-

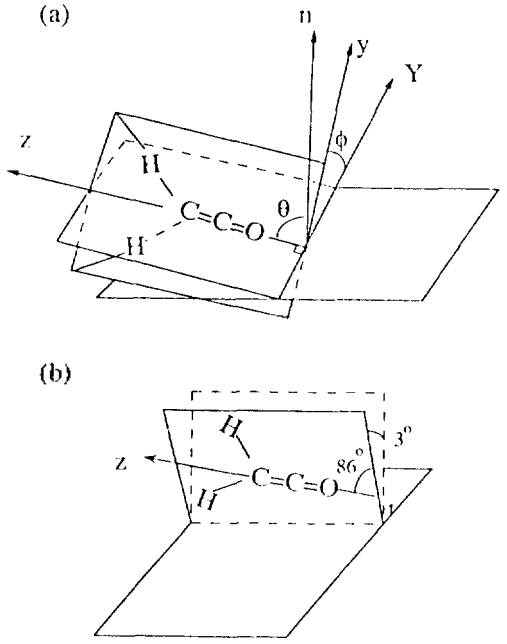

Figure 4. (a) Coordinate system showing the angles θ and ϕ which define the orientation of ketene on the surface (surface normal *n*). (b) Adsorption geometry of ketene on Ag(111). The angles shown are not exactly θ and ϕ in (b) but are numerically close to the values of these angles.

ching and that at 385 meV from a mixture of CH symmetric and asymmetric stretching bands. The integrated intensities of these EELS peaks as a function of exposure behave very similary to the TPD peak intensity. The change of the EEL spectral peaks intensity with exposure can be straightforwardly understood. As the exposure increases, just like in the TPD experiment, these peaks from the first adsorbed layer becomes saturated around 3 L exposures and there is no indication of multilayer formation. The positions of these vibrational peaks differ from the corresponding gas-phase values by only a few millielectron volts, consistent with the physisorption behavior of CH_2CO on the surface.

Adsorption geometry. The integrated intensity of the individual adsorption bands of the gas phase ketene in the IR region have been experimentally measured. These IR band intensities reveal the relative strength of the transition moments of the vibrational bands. It is assumed here that the vibrational transition moments of the physisorbed molecule are the same as the gas-phase molecule. The EEL spectral intensity, under the dipole scattering selection rules, of an adsorbate on metal surfaces derives from the perpendicular component of the transition moment. Thus, comparing the EEL intensities and the gas-phase IR intensities reveal the orientation angles of ketene on the Ag(111) surface. The detailed procedure of this analysis has been demonstrated on H_2CO/Ag(111) in Ref. 13. Here, the application on CH_2CO/Ag(111) is briefly described.

The adsorption geometry of the ketene molecule is illustrated in Figure 4a, where two angles θ and ϕ define the molecular orientation. The *z*-axis in the molecular frame is along the CCO bonds of ketene and the *y*-axis is in the molecular plane but perpendicular to the CCO bonds. θ is the tilt angle between the molecular *z*-axis and the surface normal *n*, while ϕ is the rotational angle of the molecular plane defined between the molecular plane *y*-axis and the surface *Y*-axis.

Table 2. Symmetry (C_{2v} point group), direction of transition dipole moment vector μ (*x*, *y*, or *z* direction in the molecular frame), and geometrical factor G relating $\mu_\perp$ to μ ($\mu_\perp = G\mu$) for each of the nine vibrational modes

Assignment	Symmetry	Direction of μ	G
ν_1	A_1	*z*	cosθ
ν_2	A_1	*z*	cosθ
ν_3	A_1	*z*	cosθ
ν_4	A_1	*z*	cosθ
ν_5	B_1	*x*	sinθcosϕ
ν_6	B_1	*x*	sinθcosϕ
ν_7	B_2	*y*	sinθsinϕ
ν_8	B_2	*y*	sinθsinϕ
ν_9	B_2	*y*	sinθsinϕ

The ratio of the intensities of two EEL vibrational peaks in the same spectra can be related to the corresponding gas-phase IR intensity ratio by,

$$(\nu_i/\nu_j)^3(I_i^E/I_j^E) = (I_i^{IR}/I_j^{IR})(G_i/G_j)^2, \quad (2)$$

here *G* is the geometrical factor defining the projection of the transition diploe moment vector μ onto the surface normal. ν_i and ν_j are vibrational frequencies, I_i^{IR} and I_j^{IR} the integrated intensities of the gas-phase IR spectral peaks, and I_i^E and I_j^E the integrated intensities of the EEL spectral peaks.[13,21]

Table 2 shows for each of the nine vibrational modes of ketene its symmetry representation in the C_{2v} point group, the direction of μ for the fundamental band, and the associated geometrical factor *G*. From the intensity ratios, G_i/G_j and subsquently θ and ϕ can be determined.

This procedure is only applicable to vibrational modes that are dipole active in EELS. It is not useful for modes that are detected through impact scattering. To confirm that the vibrational modes of ketene on Ag(111) are dipole active, EEL spectrum was performed at several different angles off the specular direction. The contribution to off-specular intensity from dipole scattering should decrease with angle in proportion to the elastic peak intensity. The contribution from impact scattering, on the other hand, should remain constant with angle. It was found that the absolute count rate for all the vibrational peaks was observed to fall off rapidly as the scattering angle was moved off-specular, indicating that the dipole-scattering mechanism dominates in the specular direction for all the vibrational modes. Figure 5 shows the change of the EEL peaks intensity as a function of the off-specular angle for 2 L exposure of CH_2CO on Ag(111) at 87 K. The fraction of the specular intensity of each vibrational peak due to dipole scattering, D, can then be determined and incorporated as a correction to I_i^E in Equation (2).

The spectrum of 2 L exposure of ketene (0.55 θ_S) is used in the determination of the orientation angles. From the intensity ratios of the $\nu_1+\nu_7$, ν_2 and $\nu_5+\nu_6$ modes, the orientation angles are determined to be $\theta = 86° \pm 1°$ and $\phi = 87° \pm$

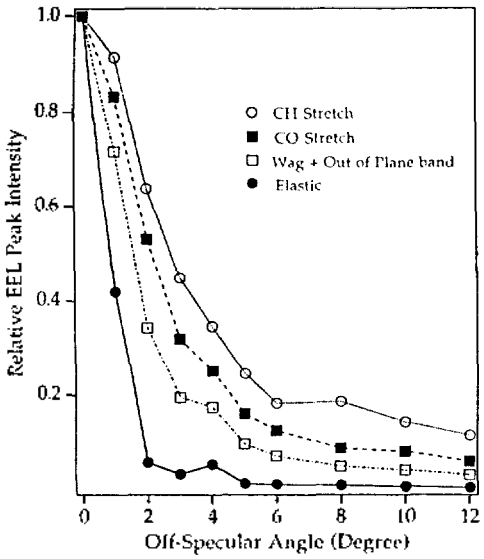

Figure 5. Vibrational EELS intensity of CH_2CO (2 L exposure) adsorbed on Ag(111) at 87 K as a function of the off-specular reflection angle.

Table 3. Dipole-scattering contribution and relative intensity of the EELS vibrational peaks of CH_2CO (2 L exposure) on Ag(111)

Peak modes	Vibrational energy (meV)	Relative EELS Intensity	D	Relative IR Intensity
$\nu_1+\nu_7$	385	1	0.85	1*
ν_2	263	1.3	0.92	13.0
$\nu_5+\nu_6$	78	10.9	0.96	8.1
ν_3	165	<0.21	0.93	0.44
ν_4	139	<0.25	0.93	0.51
ν_8	119	<0.38	0.94	–

*The ν_7 intensity in the gas-phase IR spectrum is much weaker and accounts for at most 15% of the total IR $\nu_1+\nu_7$ intensity.

1°. The ranges are determined by using a 10% uncertainty in the intergrated spectral peak intensity of both EEL and IR peaks. These angles are confirmed when intensities of ν_3 and ν_4 are used. Figure 4b shows the adsorption geometry of ketene on Ag(111).

The tilting of the CCO axis of ketene away from the surface can be confirmed simply by examining the vibrational EEL spectra and applying the selection rule for dipole scattering. The CCO axis can not be perfectly parallel to the surface since the intensity of the A_1 modes (ν_1, ν_2, ν_3, ν_4), with their transition dipole moment parallel to the CCO bond axis, are not zero. But since non-A_1 modes are also present, CCO axis should not be perpendicular to the surface either. Furthermore, a similar symmetry consideration depicts that angle ϕ is not zero. If angle ϕ is equal to zero, the B_2 modes (ν_7, ν_8, ν_9) would have zero intensity in the dipole scattering mechanism. The ν_8 peak at 119 meV is present. It is also clear that both ν_1 and ν_7 contribute to the peak at 385 meV, since the width of this peak is significantly greater than those of the other peaks in the vibrational spectra. In fact, the ν_7 mode with weak IR intensity makes the dominant contribution to the 385 meV EEL peak, since ν_1 should behave like ν_2 and does not contribute significantly to the EEL peak. Thus, ϕ should be close to 90°. Even though ϕ is large, the B_1 modes, ν_5 and ν_6, may still have intensities much larger than the other modes. This is mainly because the frequency factors strongly favour lower frequency modes in EELS.

The ketene oxygen atom with the lone-pair electrons is expected to bind more strongly to the silver surface than the hydrogen atoms. The observed 4 meV shift of the EELS CO stretching band relative to the gas-phase value supports this conjecture. The large tilt angle ($\theta=86°$) between the Ag(111) surface normal and the CCO axis probably represents a surface bonding configuration that maximizes the overlap not only with the oxygen lone pair orbitals but also with the CC π orbital as well as the CO π orbital. The CCO axis tilt angle is much larger than the 57° tilt angle of the formaldehyde CO axis away from the Ag surface normal. In formaldehyde, there is only one π orbital for interacting with Ag, thus the molecule is in a configuration maximizing both the π orbital-surface and oxygen n orbitals-surface interaction.

The angle $\phi=87°\pm1°$ obtained from the calculation indicates that the molecular plane of ketene is almost perpendicular to the Ag surface. This geometry could result from the need to maximize interaction between both oxygen n orbitals and silver in addition to the CCO π orbitals. This point becomes clear when the ketene ϕ angle is compared with the formaldehyde ϕ angle on Ag(111). For formaldehyde, ϕ was determind to be $\phi=24°\pm11°$ *i.e.* formaldehyde y-axis is almost parallel to the surface Y-axis. This geometry allows both oxygen n orbitals in the formaldehyde plane to interact with the silver surface. However, in ketene, the oxygen n orbitals are perpendicular to the molecular plane. Thus, the ketene plane has to be perpendicular to the silver surface to facilitate the oxygen n orbitals-surface interaction. The slight tilt (3°) of the molecular plane away from the perpendicular plane is most likely due to large-amplitude restricted rotational motion around the CCO axis, causing a time-averaged tilted structure.

The change of the orientation angles at different coverages have also been investigated. Using the same dipole scattering D parameters experimentally deduced for 2 L exposure, we have used the EEL spectra taken at 0.14 θ_S and 0.27 θ_S to caculate the angles at low coverages and those at 6 L and 10 L exposures for near saturation coverages. It was found that the θ angle changes from 88° at low coverages, to 86° at 0.55 θ_S and eventually to 85° at θ_S. The slightly more tilted structure away from the surface could be a result of crowding near saturation coverage. The ϕ angle also changes slightly from 88° at low coverages to 86° near saturation, although the changes are within the uncertainty of the calculation.

Summary

From the temperature programmed desorption spectra and vibrational EEL spectra, we have deduced that ketene is physisorbed on the Ag(111) surface at temperatures below 126 K. At 87 K ketene coverage on surface increases linearly with exposure until saturation at ~4 L. TPD results show

that there is no multilayer formation and no shift in the peak desorption temperature is observed, indicating a lack of attractive interactions between the adsorbate molecules. The desorption activation energies is estimated to be 7.8 kcal/mol assuming first order desorption kinetics and a pre-exponential factor of 10^{13} s^{-1}. The vibrational EEL spectra peaks of ketene on Ag(111) match those of the gas-phase IR spectra to within a few meV, showing that the Ag surface only weakly perturbs the molecular motions.

The geometry of physisorbed ketene on Ag(111) can be determined from a comparison of the relative intensities of the vibrational EELS peaks with the gas-phase IR spectral peaks. It is found that in the time-averaged position the CCO axis of ketene is nearly lying flat on the surface (tilted 86° from the surface normal), and the molecular plane is slightly rotated away (3°) with respect to the surface normal. This geometry may allow optimum interaction of the metal surface with both the oxygen lone-pair orbitals and the two CCO π-bonding orbitals of ketene.

Acknowledgment. This work is supported by the National Science Foundation, MRL Program, under grant DMR 91-20668. J. S. Kim thanks Dr. Louise Fleck and Ms. Pui-Teng Howe for technical assistance.

References

1. Fischer, F.; Trospch, H. *Brennst. Chem.* **1926**, *7*, 97.
2. Blyholder, G.; Emmett, P. H. *J. Phys. Chem.* **1959**, *63*, 962 and **1960**, *64*, 470.
3. Brady III, R. C.; Pettit, R. *J. Am. Chem. Soc.* **1980**, *102*, 6181 and **1981**, *103*, 1287.
4. McBreen, P. H.; Erley, W.; Ibach, H. *Surf. Sci.* **1984**, *148*, 292.
5. Radloff, P. L.; Mitchell, G. E.; Greenlief, C. M.; White, J. M. *Surf. Sci.* **1987**, *183*, 377 and 403.
6. Menderson, M. A.; Radloff, P. L.; White, J. M. *J. Phys. Chem.* **1988**, *92*, 4111 and 4120.
7. Ho, W. in Desorption Induced by Electronic Transitions, DIET IV, Eds. Betz, G.; Vargar, P. (Springer-Verly, Berlin, 1990), p 48.
8. Zhou, X. L.; Zhu, X. Y.; White, J. M. *Surf. Sci. Rep.* **1991**, *13*, 73.
9. Ying, Z. C.; Ho, W. *J. Chem. Phys.* **1991**, *94*, 5701.
10. Avery, N. R. *Surf. Sci.* **1983**, *131*, 501.
11. Anderson, S.; Nybery, C.; Tengstäl, C. G. *Chem. Phys. Lett.* **1984**, *104*, 305.
12. Demuth, J. E.; Christman, K.; Sanda, P. N. *Chem. Phys.* **1982**, *76*, 3860.
13. Fleck, L. E.; Ying, Z. C.; Feehery, M.; Dai, H. L. *Surf. Sci.* **1993**, *296*, 400.
14. Golze, M.; Grunze, M.; Hirshwald, W. *Vacuum* **1981**, *31*, 697.
15. Niemantsverdriet, J. M.; Markert, K.; Wandelt, K. *Appl. Surf. Sci.* **1988**, *31*, 211.
16. Tracy, J. C. *J. Chem. Phys.* **1972**, *56*, 2748.
17. Peterson, L. D.; Kevan, S. D. *J. Chem. Phys.* **1991**, *94*, 2281.
18. (a) Borguet, E.; Dai, H. L. *J. Chem. Phys.* **1994**, *101*, 9080. (b) Borguet, E.; Ph.D Thesis, Univ. of Pennsylvania 1993.
19. Redhead, P. A. *Vacuum* **1962**, *12*, 203.
20. (a) Allen, W. D.; Schaefer III, H. F. *J. Chem. Phys.* **1988**, *89*, 329. (b) Moore, C. B.; Pimentel, G. C. *J. Chem. Phys.* **1963**, *38*, 2816. (c) Arendale, W. F.; Fletcher, W. H. *J. Chem. Phys.* **1957**, *26*, 793.
21. Ibach, H.; Mills, D. L. Electron Energy Loss Spectroscopy and Surface Vibrations (Academic Press, New York, 1982).